Differential cross sections for $H+D_2 \rightarrow HD(v'=1, J'=1,5,8)+D$ at 1.7 eV

Félix Fernández-Alonso, Brian D. Bean, and Richard N. Zare[a)]
Department of Chemistry, Stanford University, Stanford, California 94305

(Received 8 March 1999; accepted 22 April 1999)

A 1:4 mixture of HBr and D_2 is expanded into a vacuum chamber, fast H atoms are generated by photolysis of HBr ca. 210 nm, and the resulting HD (v', J') products are detected by $(2+1)$ resonance-enhanced multiphoton ionization (REMPI) in a Wiley–McLaren time-of-flight spectrometer. The photoloc technique allows a direct inversion of HD (v', J') core-extracted time-of-flight profiles into differential cross sections for the $H+D_2 \rightarrow HD(v'=1, J'=1,5,8)+D$ reactions at collision energies ca. 1.7 eV. The data reveal a systematic trend from narrow, completely backward scattering for HD ($v'=1$, $J'=1$) toward broader, side scattering for HD ($v'=1$, $J'=8$). A calculation based on the line of centers model with nearly elastic specular scattering accounts qualitatively for the observations. © *1999 American Institute of Physics.* [S0021-9606(99)01527-5]

I. INTRODUCTION

The measurement of product angular distributions from chemical reactions constitutes one of the most sensitive ways of probing the dynamics of elementary chemical events.[1–6] This measurement is even more powerful if, in addition, it is possible to attain quantum-state resolution of the scattered product. When possible, the study of angular distributions as a function of both the collision energy and the internal state of the products can be used very effectively to reach a better understanding of the forces leading to the making and breaking of chemical bonds.

In the past two decades, much effort has been put into the measurement of state-resolved differential cross sections for the $H+H_2$ exchange reaction and its isotopic counterparts.[7–9] Even though this system is the simplest neutral bimolecular reaction, and also the most thoroughly studied one from a theoretical point of view, a large body of experimental data to contrast against the most accurate scattering calculations is still lacking. Reasons include: a small total reaction cross section (1–2 Å^2);[10–13] a large number (>25) of rovibrational product states populated with cross sections on the order of 10^{-2}–10^{-3} Å^2; the need for UV, VUV, or Raman detection techniques to probe the reaction products; and the difficulty to measure not only the product yield into a particular quantum state but also to obtain angular information of sufficient resolution from such data.

The early differential cross-section measurements of Götting, Mayne, and Toennies,[14,15] Buntin, Giese, and Gentry,[16,17] and Continetti, Balko, and Lee[18] using crossed molecular beams attained vibrational state resolution of the diatomic product. From this work, it was found that the diatomic product scattered preferentially in the backward hemisphere, but there was a tendency to move toward side scattering as the collision energy was increased from threshold.

More recently, Schnieder *et al.*[19] have made the first systematic study of the hydrogen exchange reaction with rotational resolution at 1.28 and 0.53 eV using hydrogen iodide (HI) photolysis at 266 nm and D-atom Rydberg time-of-flight detection. In their work, the dependence of the differential cross section on the internal rovibrational state of the diatomic product was seen for the first time, providing a stringent test of the most detailed reactive scattering calculations presently available at these collision energies.

Work at higher collision energies has been also performed by Schnieder and co-workers at 2.2 eV[20,21] and 2.67 eV,[22] and by Xu *et al.* at 2.2 eV.[23] The work of Schnieder and co-workers at these high collision energies, however, lacks the internal energy resolution of the lower-energy experiments, making the interpretation of D-atom kinetic energy spectra more difficult. Xu *et al.* have measured the differential cross section at 2.2 eV for HD ($v'=4$, $J'=3$) using HD Rydberg-tagging detection and impulse extraction time-of-flight spectrometry. Subsequent QCT calculations carried out by Aoiz *et al.*[24] at this collision energy qualitatively agreed with the results for this particular rovibrational state. Aside from the work mentioned above, we are not aware of measurements of rotationally resolved differential cross sections for the title reaction above 1.29 eV, particularly in regard to the dependence of the differential cross section on final rotational angular momentum of the diatomic product.

Considerable interest exists at present in high collision energy measurements for this reaction system. In principle, the QCT calculations already employed at lower collision energies with reasonable success to predict integral[25–34] and differential cross sections[28,30,35,36] should become more accurate. As the collision energy is increased, the effects of zero-point energy and nonclassical behavior generally become less prominent. As a result, the classical motion of the nuclei on an accurate electronic potential energy surface (i.e., LSTH,[37,38] DMBE,[39] BKMP1,[40] and BKMP2[41]) should faithfully reflect the collision dynamics, provided that complications arising from nonadiabatic coupling to higher potential energy surfaces can be safely neglected.

Nevertheless, while QCT calculations could grasp the

a)Electronic mail: zare@stanford.edu

overall dynamical features of this reaction, comparison of these calculations with rotationally resolved differential cross-section measurements should provide the most stringent test of current computational methods for this particular reaction system. For example, theory[29,42,43] and experiment[44–48] agree that the hydrogen exchange reaction is largely adiabatic in regard to translation and vibration, i.e., translational (vibrational) energy in the reagents is efficiently converted into translational (vibrational) energy of the products. Therefore, our current ability to measure angular distributions for highly excited rovibrational states provides a further test of both approximate and exact dynamical theories on this reaction system for product states where unexpected effects may arise.

In addition, recent work by Kuppermann and co-workers[49–54] on the effect of the geometric phase on the reactivity for the hydrogen exchange reaction predicts that the importance of this phenomenon is already manifest at collision energies much lower than the lowest conical intersection energy of 2.72 eV. Calculations on the $H+D_2$ reaction at 1.29 eV already reveal some differences in the angular distributions, especially if rotational resolution of the HD product is possible.[53] However, careful experiments between 1.27 and 1.30 eV carried out recently by Schnieder and co-workers[55] could not find any trace of the resonance behavior predicted by quantum mechanical calculations on the LSTH surface incorporating the effects of the geometric phase. Additional theoretical work at a total energy of 1.8 eV for the $D+H_2$ reaction[52] concluded that geometric phase effects are already quite large and are likely to increase with collision energy as more indirect trajectories encircling the conical intersection contribute to the reactive scattering amplitude, ultimately leading to nonclassical interference effects.

We report here measurements of the angular distributions for $H+D_2 \rightarrow HD(v'=1, J'=1,5,8)+D$ at a collision energy of 1.7 eV using the photoloc technique. It is our hope that these measurements will foster further theoretical investigations at high collision energies where relatively little is known about this reaction system.

II. EXPERIMENTAL SETUP

The experimental setup and time-of-flight characterization have been described in detail in a previous publication.[56] Here, we restrict ourselves to a brief account of the apparatus and the salient features of the experimental method followed in this particular work.

A 1:4 HBr (Matheson, 99.8% purity) and D_2 (Cambridge isotope Laboratories, 99.8% purity) mixture held at a stagnation pressure of 300 Torr in a passivated reagent manifold is expanded into a vacuum chamber with a pulsed solenoid valve (General Valve Corporation, series 900, 0.5 mm orifice) operating at 10 Hz. Typical gas pulses, as measured by monitoring D_2 $E,F\,^1\Sigma_g^+ - X\,^1\Sigma_g^+$, and HBr $H\,^1\Sigma^+ - X\,^1\Sigma^+(2+1)$ REMPI ion signals, are approximately 600 μs. The pulsed solenoid valve injects the gas pulse into the extraction region of a Wiley–McLaren time-of-flight spectrometer[56] at nominal pressures of $5.0-10.0 \times 10^{-6}$ Torr. It is in this region that reaction takes place.

The linearly polarized output of a dye laser (Lambda Physik SCANMATE 2E) pumped by the second harmonic of an injection-seeded Nd:YAG laser (Spectra Physics GCR-4) is doubled and mixed in BBO crystals to reach 208–220 nm. Typical output powers in the UV are between 0.5–1.5 mJ/pulse with pulse durations of 5–6 ns as measured with a fast photodiode (ET 2000). The UV output is efficiently separated from the fundamental and doubled beams by the use of dichroic mirrors (CVI Corporation). The beam is sent through a 3:1 Galilean telescope prior to being focused by a 600 mm fused silica plano-convex lens to enhance beam focusing, and through a set of two UV polarizers (CVI Corporation) for fine control of the laser power. The state of polarization of the beam is controlled by the use of a half-wave plate (Optics for Research) mounted on a rotatable optical stage.

In the experiments described in this paper, the same laser is used to photolyze HBr and to detect the resulting reaction products created within the laser temporal pulse width (5–6 ns). In this regime, it is safe to neglect effects caused by fly-out of the reaction product, as it has already been shown in past integral cross-section measurements in our laboratory.[57–59] The laser beam traverses the vacuum chamber perpendicular to both the nozzle and time-of-flight axis. Chemical reaction occurs at 25–35 nozzle diameters away from the nozzle exit. From measurements of the D-atom yield of the chemical reaction and by comparison with D-atom signals arising from DBr impurity, we have estimated that the local pressure in the beam is less than 1 millitorr, corresponding to a mean free path of at least 0.5 m in the reaction region. We have further checked for secondary collisions affecting the velocity distributions by recording time-of-flight profiles at different nozzle distances and determining under which conditions the experimental data correspond to a nascent distribution.

HD (v', J') product molecules are detected via $(2+1)$ REMPI in a quantum-specific manner using the Q-branch members of the HD $E,F\,^1\Sigma_g^+ - X\,^1\Sigma_g^+(0,1)$ band.[60,61] This detection scheme is largely insensitive to the rotational polarization of the HD product, as evidenced by the dominant contribution of the zero-rank tensor term in the line strength expression.[62–64] Consequently, HD^+ ion intensities can be directly related to ground-state populations. HD^+ ions are then extracted into the acceleration and free-drift regions of the time-of-flight apparatus, core-extracted by a 3 mm conical mask (Beam Dynamics Inc.), and detected with a chevron-type, multichannel-plate detector (Galileo Corporation) held at 2.0–2.3 kV. Ion signals are recorded on a digital oscilloscope (Tektronics TDS 620) and sent via a GPIB interface (National Instruments) to a personal computer (Pentium 133 MHz) for further analysis.

III. RESULTS

Table I summarizes the reaction parameters for the $HD(v'=1, J')$ states pertinent to this work. Because we are using the same laser to photolyze and detect the HD product,

TABLE I. Summary of reaction parameters.

	HD ($v'=1$) Product		
	$J'=1$	$J'=5$	$J'=8$
Collision energy (eV)	1.71	1.70	1.66
Center-of-mass speed (m/s)	4059	4028	3986
D_2 vibrational energy (eV)	0.191	0.191	0.191
D_2 rotational energy (eV)	0.005	0.005	0.005
HD vibrational energy (eV)	0.683	0.683	0.683
HD rotational energy (eV)	0.011	0.156	0.364
HD center-of-mass speed (m/s)	5497	5086	4432
HD laboratory speed (m/s)			
Fast	9556	9114	8418
Slow	1439	1057	446

the collision energy varies slightly from 1.71 eV for $J'=1$ to 1.66 for $J'=8$. This change in collision energy is still within the collision energy spread of 0.05 eV[56] inherent in these experiments. The collision energy spread corresponds to an upper limit obtained from measurements of the translational temperatures of the reagents ($\sim$50 K), and the rotational distribution of the D_2 reagent. The D_2 reagent distribution has been measured by $(2+1)$ REMPI and corresponds to 0.45:0.35:0.10 in the $J=0,1,2$ levels of the ground vibrational level.

The center-of-mass and laboratory speeds of the HD products are listed in the last two rows of Table I. Accounting for the photolysis branching ratio,[56,65] the different rate constants for reaction,[66] and the detection geometry, the contribution of the slow photolysis channel is not more than 10%–15% of the total signal in the worst case scenario.

Figure 1 shows typical core-extracted time-of-flight profiles for the three rovibrational states pertinent to this work. The profiles for HD ($v'=1$, $J'=5$) and HD ($v'=1$, $J'=8$) were obtained at an extraction voltage of 50 V, whereas that for HD ($v'=1$, $J'=1$) required, because of small signal levels, an extraction voltage of 100 V. This increase in extraction voltage from 50 to 100 V translates into a twofold temporal compression of the ion packet. For ease of comparison with the other two time-of-flight profiles, the time axis for HD ($v'=1$, $J'=1$) has been expanded by a factor of 2. With the experimental data plotted in this manner, a given time-of-flight shift from zero corresponds to the same speed along the time-of-flight axis for all three profiles shown.

Each profile is the result of counting all the ions arriving at m/e=3 during 20 000 laser shot intervals. All three profiles were recorded with the laser polarization perpendicular to the time-of-flight axis. The signals were carefully checked for experimental artifacts including improper centering of the core extractor and space-charge effects arising from the concomitant production of Br^+ and HBr^+ ions.

The solid line accompanying each profile is the result of a linear least-squares fit using a total of 12 evenly spaced velocity basis functions. The fit was performed via both a singular-value decomposition[67] and a maximum entropy plus simulated annealing algorithm.[68–70] The results from either fitting procedure are indistinguishable within the error of our measurements. The core-extracted velocity basis functions were generated via a Monte Carlo simulation of the instrument. The instrumental calibration parameters have been described in detail in a previous publication, and therefore the details will be omitted.[56]

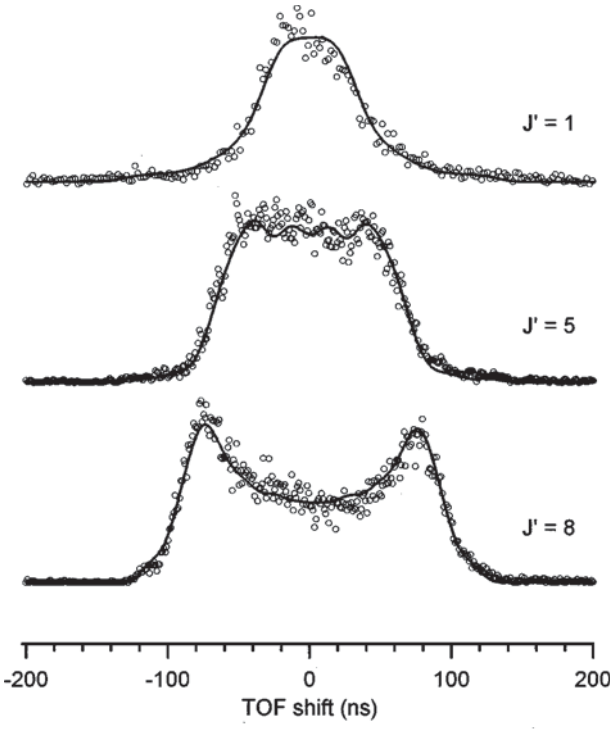

FIG. 1. Core-extracted time-of-flight profiles for H+D$_2$→HD($v'=1, J'=1,5,8$)+D at collision energies ca. 1.7 eV. HD detection was accomplished by $(2+1)$ REMPI through the Q-branch members of the HD $E,F\,^1\Sigma_g^+ - X\,^1\Sigma_g^+(0,1)$ band. The solid lines are least-squares fits to the experimental profiles using the methods described in the text. For clarity the profile for $J'=1$, taken at half the velocity resolution, has been expanded by a factor of 2 along the abscissa.

Each laboratory velocity of the HD product corresponds to a unique scattering angle in the center-of-mass frame according to the law of cosines

$$v_{AB}^2 = u_{\mathrm{CM}}^2 + u_{AB}^2 + 2\cdot u_{\mathrm{CM}}\cdot u_{AB}\cdot \cos\theta_r, \tag{1}$$

where θ_r is the center-of-mass scattering angle, v_{AB} and u_{AB} are the laboratory and center-of-mass speeds of the AB product, and u_{CM} is the speed of the center of mass. The product angular distribution $P(\cos\theta_r)$ and hence the normalized differential cross section $(1/\sigma)(d\sigma/d\Omega_r)$ are then related to the measured velocity distribution $P(v_{AB})$ by a simple Jacobian transformation

$$P(\cos\theta_r) = 2\pi\frac{1}{\sigma}\left(\frac{d\sigma}{d\Omega_r}\right) = \left(\frac{u_{CM}\cdot u_{AB}}{v_{AB}}\right)\cdot P(v_{AB}), \tag{2}$$

where θ_r and v_{AB} are related to each other through the law of cosines as shown in Eq. (1).

Figure 2 shows the angular distributions derived from the core-extracted time-of-flight profiles of Fig. 1. This figure constitutes the major findings of this study. At least five measurements were performed for each rovibrational state. The 1σ error bars shown include both the statistical uncertainties arising from the linear least-squares fits as well as the systematic variations from separate measurements. We have

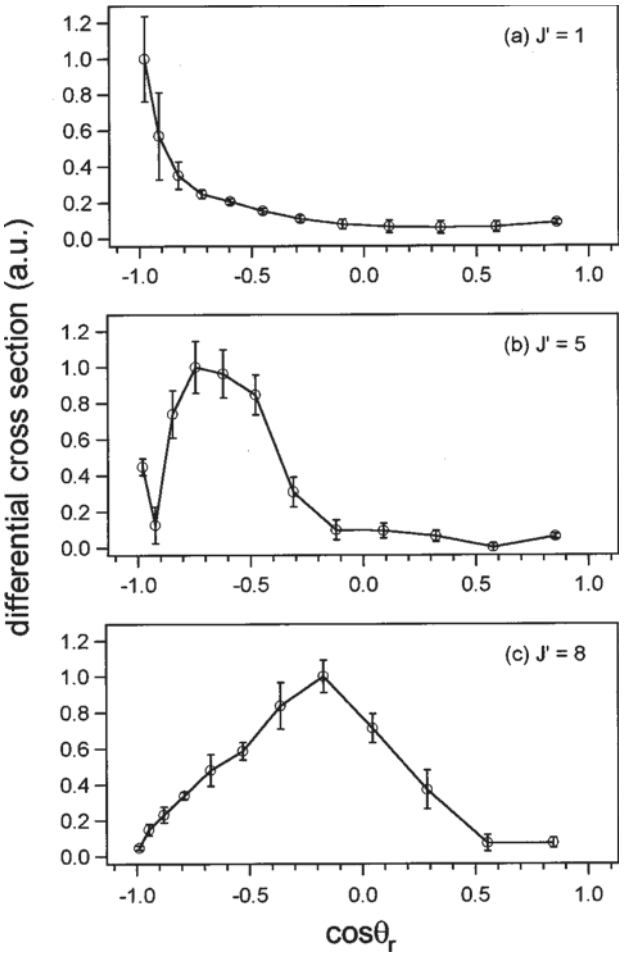

FIG. 2. Angular distributions derived from the core-extracted time-of-flight profiles shown in Fig. 1. The solid lines are guides to the eye.

estimated an angular resolution of 5–6 deg in the backward region and 12–13 deg in the forward scattering region with the current velocity resolution.

Despite these uncertainties in our measurements, the angular distributions show a marked dependence on the final rotational quantum number of the HD ($v'=1$, J') product. For $J'=1$, it peaks at ~170 deg and is quite sharp, reaching 20% of its maximal value at ~130 deg. The larger error bars in this angular distribution arise from the increased covariance between velocity basis functions as a consequence of a larger extraction voltage (i.e., worse velocity resolution) required for the measurement of this particular product state.

Figure 2(b) shows the angular distribution for $J'=5$. Its peak has shifted to ~133 deg and a broader range of angles contributes to product scattering. In addition to these coarse features, the angular distribution appears to show a local minimum at ~155 deg. This feature is present in all the time-of-flight profiles measured for this state and persists if the basis-set calibration parameters are varied over a wide range of values.

Finally, for $J'=8$ the maximum in the distribution has shifted to ~100 deg and its breadth has roughly doubled with respect to that at $J'=5$. A preference exists, however, for scattering into the backward hemisphere, as evidenced by the asymmetry of the distribution with respect to complete side scattering at 90 deg.

IV. DISCUSSION

A. Comparison with previous work

Presently, no theoretical calculations exist for this reaction at the collision energies of our experiments. In the future, it would be interesting to compare our results with theoretical calculations carried out with and without the geometric phase, because the presence of the geometric phase is predicted[51,53] to have more pronounced effects at higher collision energies than those probed in other experiments.

Comparison with the extensive theoretical and experimental work at 1.28 eV shows that, qualitatively, the reaction behaves in a very similar manner at both collision energies. The angular distributions of Schnieder *et al.*[19] for the same states we have probed peak at approximately 175, 120, and 90 deg. They also show a similar broadening of the angular distribution with rotational quantum number. Such a similarity in behavior at post-threshold collision energies suggests that, to a first-order approximation, the same dynamics determine the measured distributions.

B. Line-of-centers nearly elastic specular scattering (LOCNESS) model for $H+H_2$ dynamics

Before suggesting an interpretation of the results described in Sec. III, a few general remarks on what is known about the nature of this reaction are in order. An extensive amount of theoretical work, both classical and quantum mechanical, show the reaction is of direct character,[2,71,72] although computations[7,32,35,73,74] have provided some evidence for the possibility of more complicated behavior, such as complex formation and scattering resonances.

Very simple physical considerations can shed some light onto the claim that this reaction is direct in character. The H atom and D_2 molecules are ''small,'' with van der Waals radii on the order of a_0 ($a_0=0.529$ Å). Using a_0 as the ''characteristic'' collision radius for the $H+D_2$ reaction, we can arrive at a cross section of $\pi a_0^2=0.9$ Å^2, a value reasonably close to the calculated and measured reactive cross sections at these collision energies. Of course, this simple estimate does not capture the inherent collision energy dependence of the reaction cross section, but it predicts the right order of magnitude in regard to the nature of the reactive event. Such a small cross section also implies a narrow range of impact parameters leading to reaction, usually on the order of $b=1-2\ a_0$. These impact parameters correspond to values of the initial orbital angular momentum of $L=\mu v_{\mathrm{rel}} b/\hbar=10-20$ at our collision energies.

Consideration of the time scales for the various molecular motions involved in the reaction shows that, under our experimental conditions, in which a mixture of $J=0$, 1, and 2 reagent states is present, it is safe to neglect the effect of reagent rotation in our qualitative discussion of this reaction system. The rotational period of a D_2 ($v=0$, $J=1$) molecule is on the order of 170 fs, in contrast with a classical vibrational period of 10 fs, and a characteristic collision time of

$t_{coll}=a_0/v_{rel}=4$ fs at $E_{coll}\sim 1.7$ eV. The disparity of the time scales for rotational motion versus vibrational or translational motions allows us to treat, to a large degree of confidence, this degree of freedom as frozen. In other words, rotational effects from reorientation of the reagent during the collision can be ruled out at our collision energies. It is thus expected that the distribution of rotational levels in the D_2 $(v=0)$ reagent inherent in our experiments has little effect on the measured angular distributions. This claim is substantiated by quasiclassical trajectory calculations performed by Aoiz *et al.*[34] for the $H+D_2$ reaction at a collision energy of 1.29 eV. (Note that for collision energies approaching the reaction threshold, this behavior no longer holds. See, for example, the calculations by Aoiz *et al.*[29,34] and Truhlar *et al.*[75])

The most accurate *ab initio* calculations of the H_3 potential energy surface show a large energy dependence on the angle of attack, γ, of the incoming hydrogen atom. Here, γ is the H–D–D angle which is zero when the approach of the H atom is collinear with the D–D internuclear axis. The barrier height for reaction changes from 0.4 eV for a collinear approach to 2.0 eV[38] for a geometry where the hydrogen atom approaches the D atom from the ''wrong'' side, corresponding to an angle of attack of roughly 110 deg. From these considerations, it can be expected that there is a large preference for those trajectories that approach a collinear geometry to react. The steep dependence of the potential energy with angle γ ensures that even at collision energies as high as 1.7 eV, we can still expect to see its manifestation in the measured angular distributions. As discussed in more detail below, this preference for a collinear geometry is especially true for those collisions at large impact parameters where there is less energy along the line of centers to surmount the barrier for reaction. In this case, a smaller range of transition state geometries can therefore contribute to the reactive flux.

Having established on physical grounds the direct and geometrically constrained character of this reaction, we consider whether the measured angular distributions can be related to dynamically significant quantities. For this purpose, we use the simplest extension of the optical model to reactive scattering.[76–82] We begin by writing the total scattering angle, θ_r, for the product as a sum of reactant and product contributions, both governed by potentials of the two-body type. Because it is customary to define θ_r as the angle between the initial and final relative velocity vectors, this relationship is given by

$$\theta_r=\pi-[\theta(b,E_T)_{react}+\theta(b',E_T')_{prod}], \tag{3}$$

where we have explicitly written the dependence of the deflection angles θ_{react} and θ_{prod} on impact parameter b and relative translational energy E_T. The translational energy dependence may be removed if θ_{react} and θ_{prod} are assumed to follow hard-sphere scattering. If this hard-sphere assumption holds, then the relationship between entrance and exit angles and their corresponding impact parameters is simply given by

$$\sin\theta_{react}=b/d, \tag{4}$$

$$\sin\theta_{prod}=b'/d', \tag{5}$$

where d and d' are the hard-sphere radii characterizing the interaction between reagents and products, respectively.

Finally, in the $H+D_2$ reaction the reactant and product channels are expected to have a very similar hard-sphere diameter, i.e., $d\sim d'$, and a very similar (small) range of impact parameters in the entrance and exit channels. All these approximations lead us to the celebrated ''specular'' reflection approximation, whereby

$$\theta_r=\pi-2\arcsin(b/d), \tag{6}$$

or

$$\cos\theta_r=2\frac{b^2}{d^2}-1. \tag{7}$$

Clearly, the one-to-one correlation between impact parameters and scattering angles invoked above is generally invalid for reactive scattering. For example, for direct reactions taking place via a linear complex there exists a one-to-one relationship between b and b'. Other geometries of the transition state lead to a distribution of b' values for each initial b, with an average value approaching the linear limit.[81] For reactions in which the reaction complex is short-lived and its geometry is preferentially collinear, however, such a limit can still be qualitatively approached. We should note that a very similar argument has already been used by Kwei and Herschbach[83] to predict the product total angular distribution for the $H+H_2$ and $D+H_2$ reactions.

The HD $(v'=1, J')$ differential cross-section data presented here suggest that if the line-of-centers nearly elastic specular scattering (LOCNESS) model presented above is qualitatively correct, then low-J' product states correlate with reactive collisions at small impact parameters, and high-J' states with large impact parameters. Classically, this correspondence between low-J states and backward scattering is easy to picture by taking into account the collinear character of the minimum energy path in the potential energy surface. For $b=0$, reactive collisions are preferentially head-on and of rebound character. Consequently, little torque is imparted to the emerging HD product. As b increases, the collision becomes more glancing, but the preferred geometry for the switchover between reagents and products is even more strongly collinear. In this situation, some of the initial translational energy is converted into rotational energy of the product because the H–D–D axis is not parallel to the incoming relative velocity vector at the point where reaction takes place. Figure 3 shows a ball-and-stick pictorial representation of these ideas. This figure emphasizes the fact that for large impact parameters, the range of reactive geometries is more constrained than for head-on collisions because the available energy along the line of centers, namely $E_T(1-b^2/d^2)$, decreases as b increases.

This simple and inherently classical picture for the dependence of the differential cross section on product rotation can be further refined if we consider the correlation between the initial and final angular momenta of a generic $A+BC$ reactive system, and incorporate in a semiquantitative manner kinematic and energetic constraints. As Gordon *et al.*[84,85] have argued, the $H+H_2$ reaction displays a correlation between the initial orbital angular momentum $\mathbf{L}$ and the rota-

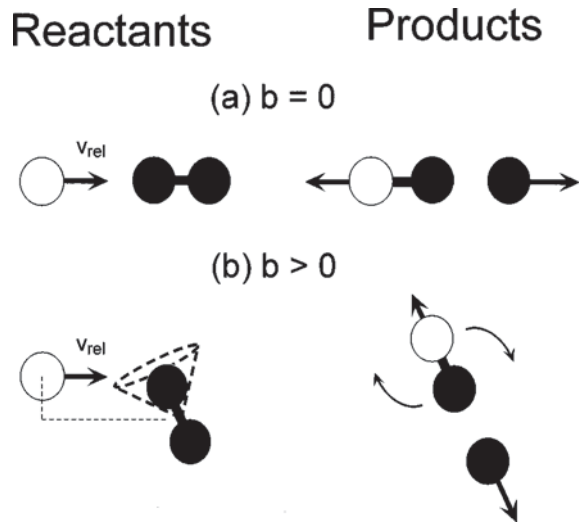

FIG. 3. Pictorial representation of the relationship between reactive impact parameter b and product rotational angular momentum J'. Panel (a) shows a zero-impact-parameter collision leading to rotationally cold, backscattered product. Panel (b) shows a large impact parameter collision leading to more rotational excitation and smaller scattering angles. Panel (b) also includes an approximate ''cone of acceptance'' for collisions leading to reactive product. The larger impact parameter necessarily implies a smaller amount of energy to surmount the angle-dependent barrier. Consequently, a narrower range of transition state geometries are energetically available.

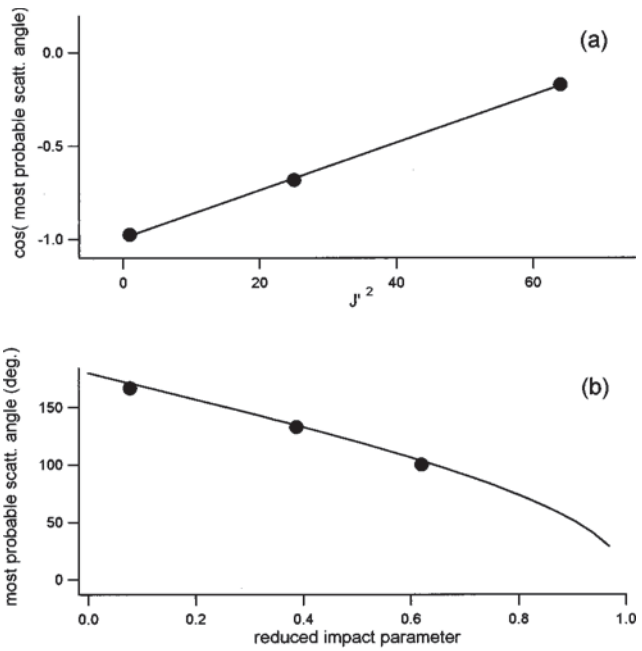

FIG. 4. (a) Correlation between the most probable scattering angle θ_{mp} and product rotational angular momentum J'. (b) Relationship between scattering angle and reduced impact parameter, b/d, deduced from the correlation shown in (a). The solid line represents the hard-sphere limit.

tional excitation of the product $\mathbf{J}'$ of the form $\mathbf{J}'=\alpha\mathbf{L}$ plus higher order terms. A rotational distribution can thus be used to derive a coarse opacity function for each product vibrational level. In our case, we go one step further and use the one-to-one relationship between impact parameter and scattering angle to examine, at least qualitatively, the J' dependence of the opacity function for this reaction. More explicitly, we can show that if Eq. (7) is correct, then the relationship between the opacity function, $P(b)$, and the angular distribution is given by

$$\frac{d\sigma}{d\cos\theta_r}=2\pi P(b)b\frac{db}{d\cos\theta_r}=P(b)\left(\frac{\pi d^2}{2}\right). \tag{8}$$

To test the rough validity of the proposed correlation between the magnitude of $\mathbf{J}'$ and impact parameter b, we have plotted in Fig. 4(a) the most probable value of the scattering angle for the angular distributions of Fig. 2 as a function of J'^2. The three states shown in this figure all fall on a straight line, in agreement with what is expected for a linear correlation between $\mathbf{J}'$ and $\mathbf{L}$, and for scattering that approaches the hard-sphere specular limit. From a linear fit of these points, we can obtain the scaling of the impact parameter with J' for this particular vibrational manifold. Figure 4(b) shows a plot of the scattering angle as a function of reduced impact parameter $b_{\mathrm{red}}=b/d$. In the same plot, we have included the three experimental most probable scattering angles as a function of the reduced impact parameter obtained from Fig. 4(a). In this case, the experimental points follow quite closely the hard-sphere functional form, which confirms the reasonability of the model. Thus, the gross behavior of the differential cross section as a function of the rotational level for the HD $(v'=1,\ J')$ product follows closely the expectations of the LOCNESS model that links the initial impact parameter with rotational excitation of the product.

C. Outlook

The relationship found between J' and b is consistent with the small amount of product rotational energy already observed for this reaction in quantum-state-resolved integral cross-section measurements. Surprisal analysis of a large body of integral cross-section data at various collision energies shows that the rotational distributions are always below the prior limit, with the fraction of the energy going into rotation never accounting for more than 25% of the total available energy.[42,44,45,47,86,87] According to our interpretation, small impact parameters contribute to the reaction; therefore, relatively ''cold'' rotational distributions should be observed. Moreover, we can use the correlation between reduced impact parameter and rotational quantum number shown in Fig. 4, and the collinear barrier to reaction, $E_0=0.4\,\mathrm{eV}$, to predict that $J'=11$ $(b_{\mathrm{red}}^2=1-E_0/E_{\mathrm{coll}})$ will be the maximum rotational quantum number possible at these collision energies for HD $(v'=1,\ J')$ product. The observation of higher product rotational quantum numbers would be indicative of other reaction mechanisms that cannot be described by the LOCNESS model proposed in Sec. IV B.

Furthermore, if we accept the qualitative correctness of the LOCNESS model put forth to explain the angular distributions, we would expect to find a similar correlation between J' and b for rotational states of other vibrational manifolds. In one sense, the angular distribution will be largely ''blind'' to the final vibrational level. For example, a $J'=0$ state should always peak at angles approaching 180 deg ir-

respective of the vibrational state of the product. It should be noted, however, that the rotational distribution should be quite dependent on the vibrational quantum number. A direct and collinearly dominated reaction mechanism implies that small impact parameter collisions, and thus low product rotational quantum numbers, are most effective at converting the relative translational energy of the reagents into vibrational excitation of the product. Corroboration of these predictions awaits further experiments.

The LOCNESS model introduced to account for the observations succeeds at explaining the behavior of the peak of the angular distribution with rotational quantum number. It does not say anything, however, about the increase in the spread of the angular distribution. Similarly, it cannot predict the shape of the angular distributions unless we are prepared to make further assumptions. A detailed comparison with theoretical predictions will require quasiclassical and quantum mechanical scattering calculations at these collision energies. Nevertheless, it is heartening how much insight into this reaction can be gained from simple classical arguments.

V. CONCLUSIONS

We have performed differential cross-section measurements for $H+D_2 \rightarrow HD(v'=1, J'=1,5,8)+D$ at 1.7 eV. The angular distributions show a marked variation with product rotational quantum number; the most probable scattering angle shifts from 170 deg for $J'=1$ to 100 deg for $J'=8$. The angular distributions also become markedly broader with product rotational quantum number. Lack of additional experimental or theoretical data at these collision energies does not allow for a direct and quantitative comparison of this study with other work at present. Qualitative comparison with the work of Schnieder *et al.*[19] at 1.28 eV reveals a similar behavior of the angular distributions at both collision energies. A simple line-of-centers model with nearly elastic specular scattering (LOCNESS) is proposed to account qualitatively for the observed trends. In this LOCNESS model, a correlation between the product J' and initial impact parameter b is assumed. The predictions of this model are not only consistent with the J' dependence of the differential cross section, but also with the current knowledge of the dynamics and energy disposal of this reaction.

ACKNOWLEDGMENTS

We thank James D. Ayers, Zee Hwan Kim, and Michael A. Everest for valuable discussions. The National Science Foundation is gratefully acknowledged for financial support under Grant No. CHE-93-22690 and CHE-99-00305.

[1] R. E. Wyatt and J. Z. H. Zhang, *Dynamics of Molecules and Chemical Reactions* (Marcel Dekker, New York, 1996).
[2] R. D. Levine and R. B. Bernstein, *Molecular Reaction Dynamics and Chemical Reactivity* (Oxford University Press, New York, 1989).
[3] M. N. R. Ashfold and J. E. Baggott, *Bimolecular Collisions* (Royal Society of Chemistry, London, 1989).
[4] D. C. Clary, *The Theory of Chemical Reaction Dynamics* (Reidel, Dordrecht, 1985).
[5] D. G. Truhlar, *Potential Energy Surfaces and Dynamics Calculations for Chemical Reactions and Molecular Energy Transfer* (Plenum, New York, 1981).
[6] R. B. Bernstein, *Atom-Molecule Collision Theory: A Guide for the Experimentalist* (Plenum, New York, 1979).
[7] W. H. Miller, Annu. Rev. Phys. Chem. **41**, 245 (1990).
[8] H. Buchenau, J. P. Toennies, J. Arnold, and J. Wolfrum, Ber. Bunsenges. Phys. Chem. **94**, 1231 (1990).
[9] R. D. Levine, Int. J. Chem. Kinet. **18**, 9 (1986).
[10] K. Tsukiyama, B. Katz, and R. Bersohn, J. Chem. Phys. **84**, 1934 (1986).
[11] G. W. Johnson, B. Katz, T. Tsukiyama, and R. Bersohn, J. Phys. Chem. **91**, 5445 (1987).
[12] U. Gerlach-Meyer, K. Kleinermanns, E. Linnebach, and J. Wolfrum, J. Chem. Phys. **86**, 3047 (1987).
[13] R. A. Brownsword, M. Hillenkamp, T. Laurent, H.-R. Wolpp, J. Wolfrum, R. K. Vatsa, and H.-S. Yoo, J. Phys. Chem. A **101**, 6448 (1997).
[14] R. Götting, H. R. Mayne, and J. P. Toennies, J. Chem. Phys. **80**, 2230 (1984).
[15] R. Götting, H. R. Mayne, and J. P. Toennies, J. Chem. Phys. **85**, 6396 (1986).
[16] S. A. Buntin, C. F. Giese, and W. R. Gentry, J. Chem. Phys. **87**, 1443 (1987).
[17] S. A. Buntin, C. F. Giese, and W. R. Gentry, Chem. Phys. Lett. **168**, 513 (1990).
[18] R. E. Continetti, B. A. Balko, and Y. T. Lee, J. Chem. Phys. **93**, 5719 (1990).
[19] L. Schnieder, K. Seekamp-Rahn, E. Wrede, and K. H. Welge, J. Chem. Phys. **107**, 6175 (1997).
[20] E. Wrede, L. Schnieder, K. H. Welge, L. Bañares, and V. J. Herrero, Chem. Phys. Lett. **265**, 129 (1997).
[21] F. J. Aoiz and J. F. Castillo, Faraday Discuss. **110**, 215 (1998).
[22] E. Wrede, L. Schnieder, K. H. Welge, F. J. Aoiz, L. Bañares, V. J. Herrero, B. Martínez-Haya, and V. Sáez Rábanos, J. Chem. Phys. **106**, 7862 (1997).
[23] H. Xu, N. E. Shafer-Ray, F. Merkt, D. J. Hughes, M. Springer, R. P. Tuckett, and R. N. Zare, J. Chem. Phys. **103**, 5157 (1995).
[24] F. J. Aoiz, L. Bañares, and V. J. Herrero, J. Chem. Phys. **105**, 6086 (1996).
[25] N. C. Blais and D. G. Truhlar, Chem. Phys. Lett. **102**, 120 (1983).
[26] N. C. Blais and D. G. Truhlar, J. Chem. Phys. **83**, 2201 (1985).
[27] N. C. Blais, D. G. Truhlar, and B. C. Garrett, J. Chem. Phys. **82**, 2300 (1985).
[28] F. J. Aoiz, V. Candela, V. J. Herrero, and V. Sáez Rábanos, Chem. Phys. Lett. **169**, 243 (1990).
[29] F. J. Aoiz, V. J. Herrero, and V. Sáez Rábanos, J. Chem. Phys. **94**, 7991 (1991).
[30] F. J. Aoiz, L. Bañares, M. J. D'Mello, V. J. Herrero, V. Sáez Rábanos, L. Schnieder, and R. E. Wyatt, J. Chem. Phys. **101**, 5781 (1994).
[31] F. J. Aoiz, V. J. Herrero, O. Puentedura, and V. Sáez Rábanos, J. Chem. Phys. **100**, 758 (1994).
[32] F. J. Aoiz, V. J. Herrero, and V. Sáez Rábanos, J. Chem. Phys. **97**, 7423 (1992).
[33] F. J. Aoiz, H. K. Buchenau, V. J. Herrero, and V. Sáez Rábanos, J. Chem. Phys. **100**, 2789 (1994).
[34] F. J. Aoiz, V. J. Herrero, O. Puentedura, and V. Sáez Rábanos, Chem. Phys. Lett. **198**, 321 (1992).
[35] F. J. Aoiz, V. J. Herrero, and V. Sáez Rábanos, J. Chem. Phys. **95**, 7767 (1991).
[36] L. Schnieder, K. Seekamp-Rahn, J. Borkowski, E. Wrede, K. H. Welge, F. J. Aoiz, L. Bañares, M. J. D'Mello, V. J. Herrero, V. Sáez Rábanos, and R. E. Wyatt, Science **269**, 207 (1995).
[37] P. Siegbahn and B. Liu, J. Chem. Phys. **68**, 2457 (1978).
[38] D. G. Truhlar and C. J. Horowitz, J. Chem. Phys. **68**, 2466 (1978).
[39] A. J. C. Varandas, F. B. Brown, C. A. Mead, D. G. Truhlar, and N. C. Blais, J. Chem. Phys. **86**, 6258 (1987).
[40] A. I. Boothroyd, W. J. Keogh, P. G. Martin, and M. R. Peterson, J. Chem. Phys. **95**, 4343 (1991).
[41] A. I. Boothroyd, W. J. Keogh, P. G. Martin, and M. R. Peterson, J. Chem. Phys. **104**, 7139 (1996).
[42] E. Zamir, R. D. Levine, and R. B. Bernstein, Chem. Phys. Lett. **107**, 217 (1984).
[43] J. Z. H. Zhang and W. H. Miller, J. Chem. Phys. **91**, 1528 (1989).
[44] E. E. Marinero, C. T. Rettner, and R. N. Zare, J. Chem. Phys. **80**, 4142 (1984).
[45] D. P. Gerrity and J. J. Valentini, J. Chem. Phys. **81**, 1298 (1984).
[46] D. A. V. Kliner and R. N. Zare, J. Chem. Phys. **92**, 2107 (1990).

[47] D. E. Adelman, N. E. Shafer, D. A. V. Kliner, and R. N. Zare, J. Chem. Phys. **97**, 7323 (1992).
[48] D. Neuhauser, R. S. Judson, D. J. Kouri, D. E. Adelman, N. E. Shafer, D. A. V. Kliner, and R. N. Zare, Science **257**, 519 (1992).
[49] B. Lepetit and A. Kuppermann, Chem. Phys. Lett. **166**, 581 (1990).
[50] Y.-S. M. Wu, A. Kuppermann, and B. Lepetit, Chem. Phys. Lett. **186**, 319 (1991).
[51] Y.-S. M. Wu and A. Kuppermann, Chem. Phys. Lett. **201**, 178 (1993).
[52] A. Kupperman and Y.-S. M. Wu, Chem. Phys. Lett. **205**, 577 (1993).
[53] Y.-S. M. Wu and A. Kuppermann, Chem. Phys. Lett. **235**, 105 (1995).
[54] A. Kuppermann, in *Dynamics of Molecules and Chemical Reactions*, edited by R. E. Wyatt and J. Z. H. Zhang (Marcel Dekker, New York, 1996).
[55] E. Wrede and L. Schnieder, J. Chem. Phys. **107**, 786 (1997).
[56] F. Fernández-Alonso, B. D. Bean, and R. N. Zare, J. Chem. Phys. **111**, 1022 (1999).
[57] K.-D. Rinnen, D. A. V. Kliner, R. S. Blake, and R. N. Zare, Chem. Phys. Lett. **153**, 371 (1988).
[58] D. A. V. Kliner, K.-D. Rinnen, and R. N. Zare, Chem. Phys. Lett. **166**, 107 (1990).
[59] D. E. Adelman, H. Xu, and R. N. Zare, Chem. Phys. Lett. **203**, 573 (1993).
[60] K.-D. Rinnen, D. A. V. Kliner, R. N. Zare, and W. M. Huo, Isr. J. Chem. **29**, 369 (1989).
[61] K.-D. Rinnen, M. A. Buntine, D. A. V. Kliner, R. N. Zare, and W. M. Huo, J. Chem. Phys. **95**, 214 (1991).
[62] E. E. Marinero, R. Vasudev, and R. N. Zare, J. Chem. Phys. **78**, 692 (1983).
[63] C. Cornaggia, A. Giusti-Suzor, and C. Jungen, J. Chem. Phys. **87**, 3934 (1987).
[64] E. F. McCormack, S. T. Pratt, J. L. Dehmer, and P. M. Dehmer, J. Chem. Phys. **92**, 4734 (1990).
[65] P. M. Regan, S. R. Langford, A. J. Orr-Ewing, and M. N. R. Ashfold, J. Chem. Phys. **110**, 281 (1999).
[66] N. C. Blais and D. G. Truhlar, Chem. Phys. Lett. **162**, 503 (1989).
[67] W. H. Press, B. P. Flannery, S. A. Teukolski, and W. T. Vetterling, *Numerical Recipes in C* (Cambridge University Press, Cambridge, 1986).
[68] H. L. Kim, M. A. Wickramaaratchi, X. Zheng, and G. E. Hall, J. Chem. Phys. **101**, 2033 (1994).
[69] W. R. Simpson, Ph.D. thesis, Stanford University, 1994.
[70] W. R. Simpson, A. J. Orr-Ewing, T. P. Rakitzis, S. A. Kandel, and R. N. Zare, J. Chem. Phys. **103**, 7299 (1995).
[71] R. D. Levine, J. Phys. Chem. **94**, 8872 (1990).
[72] R. D. Levine and R. B. Bernstein, Chem. Phys. Lett. **105**, 467 (1984).
[73] R. D. Levine and S.-F. Wu, Chem. Phys. Lett. **11**, 557 (1971).
[74] W. H. Miller and J. Z. H. Zhang, J. Phys. Chem. **95**, 12 (1991).
[75] S. L. Mielke, D. G. Truhlar, and D. W. Schwenke, J. Phys. Chem. **98**, 1053 (1994).
[76] D. R. Herschbach, *Applied Optics*, Supplement on Chemical Lasers (1965), p. 128.
[77] D. R. Herschbach, Adv. Chem. Phys. **10**, 319 (1966).
[78] R. D. Levine and R. B. Bernstein, Isr. J. Chem. **7**, 315 (1969).
[79] R. Grice, Mol. Phys. **19**, 501 (1970).
[80] R. Grice and D. R. Hardin, Mol. Phys. **21**, 805 (1971).
[81] J. L. Kinsey, G. H. Kwei, and D. R. Herschbach, J. Chem. Phys. **64**, 1914 (1976).
[82] I. Schetchter and R. D. Levine, J. Chem. Soc., Faraday Trans. 2 **85**, 1059 (1989).
[83] G. H. Kwei and D. R. Herschbach, J. Phys. Chem. **83**, 1550 (1979).
[84] I. R. Elsum and R. G. Gordon, J. Chem. Phys. **76**, 3009 (1982).
[85] I. Schechter, R. D. Levine, and R. G. Gordon, J. Phys. Chem. **95**, 8201 (1991).
[86] K.-D. Rinnen, D. A. V. Kliner, and R. N. Zare, J. Chem. Phys. **91**, 7514 (1989).
[87] D. P. Gerrity and J. J. Valentini, J. Chem. Phys. **82**, 1323 (1985).